Assessing cyanobacterial frequency and abundance at surface waters near drinking water intakes across the United States

Megan M. Coffer [a,b,*], Blake A. Schaeffer [c], Katherine Foreman [d], Alex Porteous [d], Keith A. Loftin [e], Richard P. Stumpf [f], P. Jeremy Werdell [g], Erin Urquhart [h], Ryan J. Albert [d], John A. Darling [c]

[a] ORISE Fellow, U.S. Environmental Protection Agency, Office of Research and Development, Durham, NC, USA
[b] Center for Geospatial Analytics, North Carolina State University, Raleigh, NC, USA
[c] U.S. Environmental Protection Agency, Office of Research and Development, Durham, NC, USA
[d] U.S. Environmental Protection Agency, Office of Water, Washington, DC, USA
[e] U.S. Geological Survey, Kansas Water Science Center, Lawrence, KS, USA
[f] National Oceanic and Atmospheric Administration, National Centers for Coastal Ocean Science, Silver Spring, MD, USA
[g] Ocean Ecology Laboratory, NASA Goddard Space Flight Center, Greenbelt, MD, USA
[h] Science Systems and Applications, Inc., Ocean Ecology Laboratory, NASA Goddard Space Flight Center, Greenbelt, MD, USA

ARTICLE INFO

ABSTRACT

This study presents the first large-scale assessment of cyanobacterial frequency and abundance of surface water near drinking water intakes across the United States. Public water systems serve drinking water to nearly 90% of the United States population. Cyanobacteria and their toxins may degrade the quality of finished drinking water and can lead to negative health consequences. Satellite imagery can serve as a cost-effective and consistent monitoring technique for surface cyanobacterial blooms in source waters and can provide drinking water treatment operators information for managing their systems. This study uses satellite imagery from the European Space Agency's Ocean and Land Colour Instrument (OLCI) spanning June 2016 through April 2020. At 300-m spatial resolution, OLCI imagery can be used to monitor cyanobacteria in 685 drinking water sources across 285 lakes in 44 states, referred to here as resolvable drinking water sources. First, a subset of satellite data was compared to a subset of responses ($n = 84$) submitted as part of the U.S. Environmental Protection Agency's fourth Unregulated Contaminant Monitoring Rule (UCMR 4). These UCMR 4 qualitative responses included visual observations of algal bloom presence and absence near drinking water intakes from March 2018 through November 2019. Overall agreement between satellite imagery and UCMR 4 qualitative responses was 94% with a Kappa coefficient of 0.70. Next, temporal frequency of cyanobacterial blooms at all resolvable drinking water sources was assessed. In 2019, bloom frequency averaged 2% and peaked at 100%, where 100% indicated a bloom was always present at the source waters when satellite imagery was available. Monthly cyanobacterial abundances were used to assess short-term trends across all resolvable drinking water sources and effect size was computed to provide insight on the number of years of data that must be obtained to increase confidence in an observed change. Generally, 2016 through 2020 was an insufficient time period for confidently observing changes at these source waters; on average, a decade of satellite imagery would be required for observed environmental trends to outweigh variability in the data. However, five source waters did demonstrate a sustained short-term trend, with one increasing in cyanobacterial abundance from June 2016 to April 2020 and four decreasing.

1. Introduction

Public water systems (PWSs) delivered over 23 billion gallons of surface water per day in 2015 for domestic water use in the United States, providing freshwater for services such as drinking, food preparation, bathing, and landscaping (Dieter et al., 2018). These PWSs

---

served an estimated 283 million people in 2015, representing approximately 87% of the United States population. Cyanobacterial blooms can degrade the quality of drinking water sources, and some blooms can contain toxins, called cyanotoxins, which pose a human health risk when occurring at elevated levels in finished drinking water. Whether a bloom contains cyanotoxins or not, high levels of cyanobacteria in source water can necessitate that drinking water systems simultaneously address multiple treatment objectives including managing taste and odor concerns, cyanotoxin breakthrough, and disinfection byproduct (DBP) formation (U.S. EPA, 2016a).

In recent years, cyanobacterial blooms have resulted in several large-scale drinking water advisories. In September 2013, a cyanobacterial bloom along the western shore of Lake Erie resulted in nearly two thousand people being left without access to clean drinking water in the Carroll Township in Ohio (GLCR, 2013). Toledo, Ohio, issued a multi-day "Do Not Drink" advisory for more than 500,000 people in 2014 because of elevated cyanotoxins found in their finished drinking water (Great Lakes Commission, 2014). In 2018, the city of Salem, Oregon, was under a "Do Not Drink" advisory applying to vulnerable populations for several weeks, affecting several hundreds of thousands of people, after elevated levels of the cyanotoxins microcystins and cylindrospermopsin were found in its finished drinking water (The Novak Consulting Group, 2018).

Conventional drinking water treatment (e.g., coagulation, flocculation, filtration) has been proven effective in removing cyanobacterial cells and intracellular cyanotoxins (Szlag et al., 2015; U.S. EPA, 2016a). However, additional treatment approaches are typically necessary in the presence of extracellular toxins. Ultimately, the possibility of cyanotoxin breakthrough to finished drinking water is dependent on multiple factors, including the type and amount of toxins present as well as the treatment approaches, management, and operations drinking water treatment plants use to respond to a bloom in source waters.

PWSs may benefit from any advance knowledge regarding cyanobacterial bloom development in their source waters to prepare for, and if possible, mitigate the risks posed by blooms to finished drinking water. The implementation of early warning indicators (EWIs) has proven effective in managing cyanobacterial blooms, allowing managers to proactively make critical decisions to prevent further bloom proliferation (Pace et al., 2017; Wilkinson et al., 2018). EWIs are typically focused on measuring known drivers of cyanobacterial blooms where a certain predetermined threshold must be met before triggering the EWI.

Satellite imagery is a cost-effective and standardized monitoring technique for cyanobacterial blooms (e.g., Coffer et al., 2020, 2021; Dekker and Hestir, 2012; Hunter et al., 2009; Kahru and Elmgren, 2014; Kutser et al., 2006; Matthews and Bernard, 2015; Mishra et al., 2019; Papenfus et al., 2020; Stroming et al., 2020; Stumpf et al., 2016a,b; Urquhart et al., 2017), including for drinking water sources (Clark et al., 2017). While satellite imagery is typically not used to measure drivers of cyanobacterial blooms, it can provide consistent temporal coverage of cyanobacterial abundance and can serve a similar purpose as EWIs. Advance knowledge can alert drinking water managers to blooms in their source waters, indicating a need for cyanotoxin sampling in source and finished water. Results of that sampling could guide managers in implementing mitigation strategies in the source water itself, optimizing existing treatment approaches, or implementing additional treatment, with the goal of reducing the risk of cyanotoxins breaching the treatment system.

Motivated by concern for the effect of cyanobacterial blooms on drinking water quality, this study uses satellite imagery to assess the frequency and abundance of cyanobacteria at surface source waters for nearly 700 drinking water intakes across 44 states in the continental United States. Additionally, this study investigates the potential connection at a subset of these source waters between satellite remotely sensed data and a subset of qualitative visual observations collected under the fourth Unregulated Contaminant Monitoring Rule (UCMR 4). UCMR 4 qualitative responses assessed whether an algal bloom was visible near the intake within a month of quantitative finished drinking water sampling; this study considered a subset of these responses collected from March 2018 through November 2019. Satellite data were obtained from the European Space Agency's (ESA) Ocean and Land Colour Instrument (OLCI) onboard the Sentinel-3A satellite from June 2016 through April 2020. The following research objectives were addressed:

1 Using a subset of observable drinking water sources, assess agreement between satellite-derived cyanobacterial abundance and qualitative visual reporting of algal bloom presence and absence collected as part of UCMR 4.
2 Using satellite imagery collected at all resolvable drinking water sources, quantify average annual frequency of cyanobacterial blooms for the year 2019.
3 Using satellite imagery collected at all resolvable drinking water sources, analyze short-term trends in cyanobacterial abundance from June 2016 through April 2020.

2. Data and methods

2.1. Satellite observations

Satellite observations were obtained from OLCI onboard the Sentinel-3A satellite, launched in February 2016. OLCI offers a revisit frequency of approximately 2 to 3 days and a spatial resolution of 300 m at nadir, where nadir is defined as the point on Earth's surface directly below the satellite. Data are collected in 21 spectral bands with center wavelengths ranging from 400 to 1020 nanometers (nm). Standard OLCI Level-1B data (calibrated top-of-atmosphere radiances) were first obtained from ESA through the Copernicus program and were then processed to Level-2 imagery (surface reflectances) by the National Aeronautics and Space Administration (NASA) Ocean Biology Processing Group (OBPG; https://oceandata.sci.gsfc.nasa.gov). Following Urquhart and Schaeffer (2020) criteria for satellite pixel inclusion and exclusion, satellite pixels were quality flagged and discarded if they contained cloud cover, fell along the land-water interface, were adjacent to a land pixel, contained snow or ice, or contained mixed land and water signals. Removing pixels along the land-water interface and those adjacent to a land pixel ensures the shallowest portions of most lakes (ranging from 300 to 600 m from shore) are not considered, reducing the possibility of bottom reflectance being measured by the satellite sensor. Satellite pixels that were not quality flagged and discarded based on these criteria were considered valid.

This study focuses on the Cyanobacteria Index product (CI-cyano). The CI-cyano algorithm leverages spectral bands centered at 665 nm, 681 nm, and 709 nm to assess bloom biomass (Wynne et al., 2008), and those centered at 620 nm, 665 nm, and 681 nm as exclusion criteria to prevent the misidentification of non-cyanobacterial blooms, as reflectance at 620 nm is sensitive to phycocyanin (Lunetta et al., 2015). Graham et al. (2008) described potential distributions of cyanobacteria within the water column, which included cyanobacteria at a specific depth within the water column, cyanobacteria evenly distributed within the water column, and cyanobacteria as surface scums. Surface scums occur when cyanobacteria float on top of the water's surface and have optical properties similar to land vegetation (Kutser, 2009; Shi et al., 2017); thus, in our approach, surface scums will likely be quality flagged as mixed pixels and discarded before further analysis. Instead, the CI-cyano algorithm characterizes cyanobacteria within the upper layer of the water column, including cyanobacteria at depths of up to 2 m in clear water (Mishra et al., 2005) and less than 2 m in more turbid water (Wynne et al., 2010). Coffer et al. (2020) details the evolution of the CI-cyano including the differentiation between cyanobacterial blooms and other algae defined by Matthews et al. (2012).

Observations were aggregated into weekly composites preserving the maximum CI-cyano value for each pixel. The standard CI-cyano product

was converted to cyanobacterial abundance, in units of cells/mL, as CI-cyano $\times 10^8$ as described in Lunetta et al. (2015). This conversion factor was defined based on a relationship between the satellite-derived cyanobacterial index and surface water samples of *Microcystis* spp. cell counts in western Lake Erie. Throughout this study, a bloom detected by satellite imagery is defined as any cyanobacterial abundance that exceeds the detection limit of the sensor, which is preliminarily estimated to be between 10,000 and 20,000 cells/mL.

In the United States, CI-cyano has been validated quantitatively against cyanobacteria cell counts and chlorophyll-a across several states, including Florida, Ohio, Rhode Island, Massachusetts, New Hampshire, Vermont, Connecticut, and Maine (Clark et al., 2017; Lunetta et al., 2015); from 25 state health advisories in California, Oregon, New York, Idaho, New Jersey, Utah, and Vermont (Schaeffer et al., 2018); and as presence and absence (Mishra et al., 2021). Additionally, CI-cyano has been successfully demonstrated for state (Clark et al., 2017; Urquhart et al., 2017) and national (Coffer et al., 2020, 2021) assessments of cyanobacterial occurrence within the United States. CI-cyano has also been used by several states to issue recreational advisories; for example, the Wyoming Department of Environmental Quality issued such recreational advisories at Big Sandy Reservoir (Wyoming DEQ, 2018a), Eden Reservoir (Wyoming DEQ, 2018b), and Pathfinder Reservoir (Wyoming DEQ, 2018c). Coffer et al. (2020) also demonstrated expected seasonality via CI-cyano across 46 states.

Early iterations of the CI-cyano algorithm have been used for assessing cyanobacterial blooms in Lake Balaton, Hungary (Palmer et al., 2015), and the Caspian Sea (Moradi, 2014). Jin et al. (2017) leveraged the cyanobacteria index first defined in Wynne et al. (2008) to assess cyanobacteria presence and absence at Lakes Taihu and Chaohu in China. Other spectral index algorithms have been used to derive chlorophyll or cyanobacterial biomass based on reflectances in the red through near-infrared portions of the electromagnetic spectrum, such as the Maximum Peak Height (MPH) algorithm developed using imagery from ESA's MEdium Resolution Imaging Spectrometer (MERIS) for four

African study sites (Matthews et al., 2012; Matthews and Odermatt, 2015); the Maximum Chlorophyll Index (MCI) also developed using MERIS imagery but in waters surrounding Vancouver Island in Canada (Gower et al., 2005); and the Floating Algae Index (FAI) developed using imagery from NASA's Moderate Resolution Imaging Spectroradiometer (MODIS) in the western Yellow Sea near Qingdao, China (Hu, 2009).

There are 2196 lakes and reservoirs across 46 states in the continental United States that can be observed given the spatial resolution of OLCI (Fig. 1; Urquhart and Schaeffer, 2020). Lakes and reservoirs were required to be of sufficient size and shape to accommodate at least one 300-m water-only satellite pixel after the exclusion criteria described above. These range in size from 1.3 km^2 to over 4000 km^2, limiting this analysis to relatively large lakes and reservoirs across the United States. Hereafter, lakes and reservoirs will be referred to exclusively as lakes, and those lakes that can be observed with 300-m satellite imagery are referred to as observable lakes.

2.2. Resolvable drinking water intake locations

Surface intake locations extracted from the Safe Drinking Water Information System (SDWIS) database were previously described in Clark et al. (2017). Locations of drinking water intakes for each PWS facility are based on information contained in the SDWIS database. This assigned location will hereafter be referred to as the drinking water intake location or drinking water intake. These drinking water intakes were first subset to include just those within 100 m of an observable lake following Clark et al. (2017). A total of 877 drinking water intake locations were within 100 m of an observable lake. These locations were then subset to include just those within 900 m of a valid satellite pixel, a slight variation from Clark et al. (2017), selected to represent a minimum distance of three 300-m pixels in each direction. This left 685 drinking water intake locations, corresponding to 285 lakes across 44 states (Fig. 1). These remaining 685 drinking water intakes are referred to as resolvable drinking water intakes.
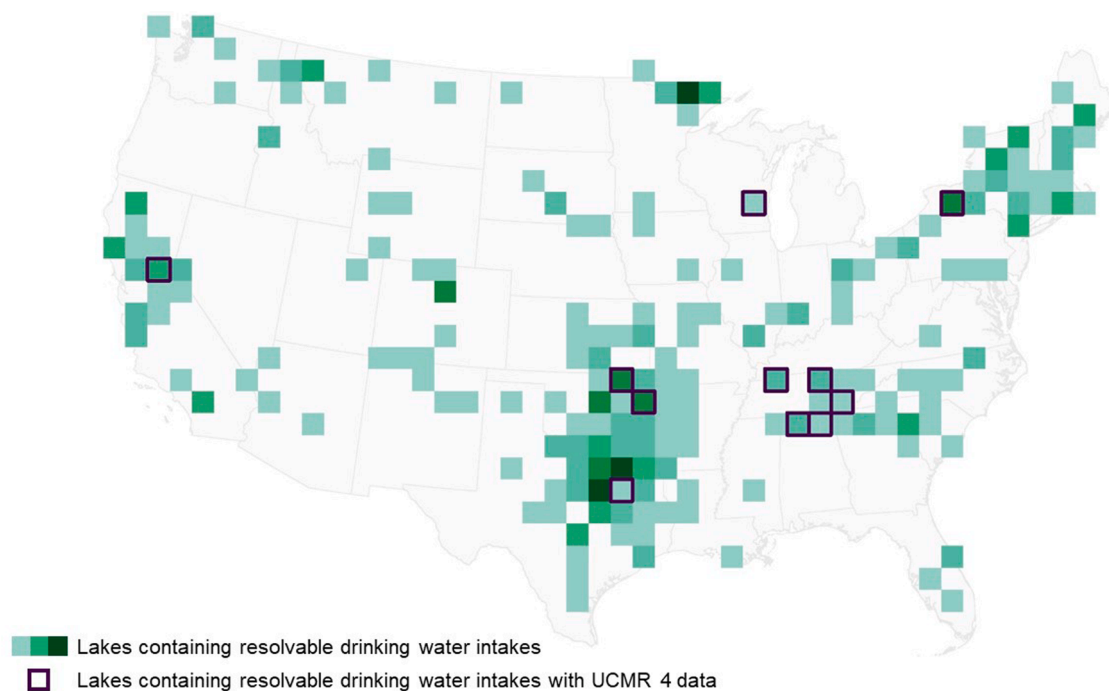

Fig. 1. A total of 285 lakes across 44 states in the continental United States contain drinking water intakes and are observable given the spatial resolution of OLCI (300 m). Green polygons indicate the density of these lakes per 100 km^2, where lighter green indicates a lower density of observable lakes per area and darker green indicates a higher density of observable lakes per area. Polygons with a purple border represent the 11 lakes across 6 states that also contain drinking water intakes where UCMR 4 qualitative responses were collected from March 2018 through November 2019. Lakes with drinking water intakes displayed in this figure are grouped spatially to protect the locations of the drinking water intakes.

Legend:
- Lakes containing resolvable drinking water intakes
- Lakes containing resolvable drinking water intakes with UCMR 4 data

Drinking water intakes that were within 100 m of an observable lake and within 900 m of a valid satellite pixel are referred to as resolvable drinking water intakes. Drinking water sources refer to the aggregated satellite pixels in an observable lake within the immediate vicinity of the drinking water intake location. For each of these resolvable drinking water intake locations, source waters were characterized by selecting all valid satellite pixels intersecting or falling within a 900-m buffer of the intake (Fig. 2).

2.3. UCMR 4 qualitative responses

The U.S. Environmental Protection Agency (EPA) collects nationally representative finished drinking water data for unregulated contaminants suspected to be present and pose a health risk in drinking water under the Unregulated Contaminant Monitoring Rule (UCMR) program (U.S. EPA, 2016b,c). This monitoring is used by the U.S. EPA to understand the frequency and level of occurrence of unregulated contaminants in the Nation's PWSs. As part of a Safe Drinking Water Act mandate, every five years the U.S. EPA develops a new list of UCMR contaminants.

UCMR 4 required monitoring for 30 chemicals between 2018 and 2020. This included monitoring for 10 cyanotoxins in finished water as well as qualitative data collected regarding the presence of an algal bloom and other characteristics in source waters around the same time as the quantitative sample collection. Cyanotoxin monitoring as part of UCMR 4 was required to be conducted twice a month for each PWS for four consecutive months, excluding the months of December, January, and February, and was required to be collected during one single year between 2018 and 2020. UCMR 4 cyanotoxin monitoring was required at all large public water systems (i.e., systems serving more than 10,000 customers) and a small, statistically representative subset of small systems that use surface water as their sources. A subset of UCMR 4 responses was obtained from the first quarter of 2020 (https://www.epa.gov/dwucmr/occurrence-data-unregulated-contaminant-monitoring-rule). Given the temporal lag between data collected by the PWS and data available for distribution, this dataset was obtained in April 2020 but only contained data from March 2018 through November 2019 and does not represent all the data collected during that timeframe.

This study is not utilizing the quantitative UCMR 4 cyanotoxin finished water data; instead it utilizes responses provided at the time of finished water monitoring in which the PWS was asked: "Preceding the finished water sample collection, did you observe an algal bloom in your source waters near the intake?" Only responses to this question of "Yes,"

"No," or "Don't know" were considered. Hereafter, these responses will be referred to as UCMR 4 qualitative responses. Some PWSs did not respond, while several PWSs recorded multiple responses over the time period. This resulted in 92 UCMR 4 qualitative responses for comparison to satellite imagery.

If the PWS responded "Yes," they were asked to specify when the algal bloom was observed. Available responses included the day the UCMR 4 cyanotoxin sample was collected, between the day the sample was collected and the past week, between the past week and the past month, between the past month and the past 12 months, and more than a year ago. Each PWS was asked to select all that applied. When PWSs responded "Yes," this study considered algal blooms observed between the day the cyanotoxin sample was collected and the past month in an effort to include as many UCMR 4 responses as possible. Including observations between the day the sample was collected and the past month can lead to limitations in the temporal matchup between UCMR 4 qualitative responses and satellite observations; however, this does not necessarily mean that satellite observations and UCMR 4 responses were one a month apart, but sometime within the previous month. Lunetta et al. (2015) found the best correspondence between satellite data and field observations of cyanobacterial abundance was within a 2-week window of the satellite overpass, which is similar to the 4-week window used here for cyanobacterial presence and absence. Additionally, it is not possible to confirm that UCMR 4 qualitative responses identified the presence of cyanobacterial blooms specifically rather than algal blooms more generally, which could lead to false positive and false negative situations when compared to satellite-derived cyanobacteria presence and absence. Despite potential temporal limitations, these visual observation responses provided via UCMR 4 are ideal for satellite comparison given that the satellite signal in our spectral region of interest also only represents the water's surface. While not a validation, this comparison is useful for assessing satellite-derived results against user perception within our target audience of PWS managers.

After identifying the drinking water intake locations corresponding to each UCMR 4 qualitative response, intake locations were subset to those identified as resolvable as described in Section 2.2. A total of 22 intakes with UCMR 4 responses from March 2018 through November 2019 corresponded to a resolvable drinking water intake location, representing 11 lakes across 6 states (Fig. 1). Low spatial coverage of UCMR 4 qualitative responses is the result of both sample design and sample reporting. While all large surface water systems were required to sample cyanotoxins in finished water as part of UCMR 4, only 800 small systems were required to sample. Additionally, not all PWS submitted qualitative
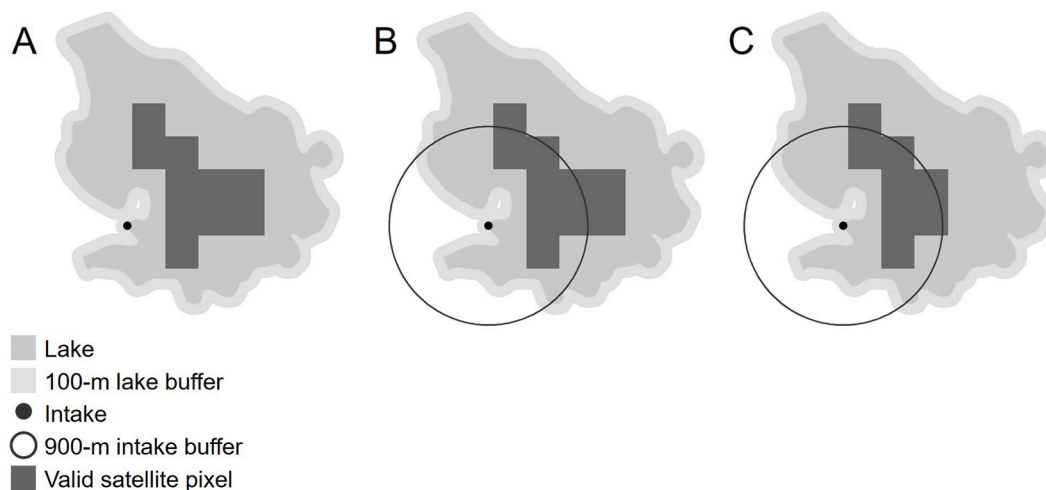

Fig. 2. A conceptual diagram illustrating data extraction at each drinking water intake location. For a drinking water intake to be considered resolvable, it must first (A) fall within a 100-m buffer of the lake boundary, and then it must (B) fall within 900 m of a valid satellite pixel. (C) All valid pixels that intersect or fall within a 900-m buffer of the intake location represent the drinking water sources and were selected for analysis.

source water data as part of their UCMR 4 finished water cyanotoxin sampling. Drinking water intakes assigned to the systems sampled then needed to correspond to a lake observable with 300-m satellite imagery and fit the selection criteria described in Section 2.3. Spatial coverage of these locations will likely improve as all UCMR 4 data becomes available.

2.4. Comparing UCMR 4 qualitative responses to satellite observations

Satellite data were extracted for each UCMR 4 qualitative response location by taking the average CI-cyano value of all valid pixels contained within a 900-m buffer of the drinking water intake as descried in Section 2.2. Each date associated with the UCMR 4 quantitative sampling was matched to the corresponding satellite weekly composite. To assess the agreement between the two datasets, two approaches were used. First, a presence-absence agreement matrix was developed to compare, on a class-by-class basis, binary satellite data and binary UCMR 4 qualitative responses. Overall agreement was computed as the number of instances that generated the same response in both satellite data and UCMR 4 qualitative responses normalized to the total number of instances considered. The Kappa coefficient was computed to indicate how well the two datasets agreed compared to a random assignment of classes (Cohen, 1960; Goodman and Kruskal, 1954). Kappa is a ratio between −1 and 1 where higher values indicate better agreement and was computed via the *fmsb* package in R version 4.0.0 (Nakazawa, 2019; R Core Team, 2020).

Next, the non-parametric Mann-Whitney U test was used to assess if cyanobacterial abundance values for UCMR 4 qualitative responses of "Yes" and "No" were generated from the same population (Mann and Whitney, 1947; Wilcoxon, 1945). A nonparametric approach is required here for several reasons: the data are not normally distributed, the sample size is relatively small, and the satellite observations contain non-detects. Cohen's d was then used to quantify the effect size (Cohen, 1992) via the *effsize* package in R version 4.0.0 (R Core Team, 2020; Torchiano, 2020), where, generally, absolute values above 0.5 indicate a "large" difference between the two means.

2.5. Assessing bloom frequency at all resolvable drinking water sources

To assess the frequency of cyanobacterial blooms at all resolvable source waters near each drinking water intake (see Fig. 2), satellite observations were aggregated into annual detections. Temporal frequency was computed per pixel following Coffer et al. (2021) as the proportion of valid satellite pixels that indicate either a detection of cyanobacteria (i.e., those above the detection limit of the sensor) or non-detection; invalid pixels are those with quality flags and were not included in the bloom frequency computation (Eq. (1)). In other words, bloom frequency is simply the cyanobacteria detected pixels divided by the total number of detect and non-detect pixels, excluding invalid quality flagged pixels. This produces a percentage between 0% and 100%, where 0% indicates no bloom was present at that pixel for the given year when satellite imagery was available and 100% indicates a bloom was always present at that pixel for the given year when satellite imagery was available. At each drinking water source, annual bloom frequency for the year 2019 represented the average bloom frequencies for all pixels contained within a 900-m buffer of each drinking water intake.

$$\text{Bloom frequency} = 100 \times \frac{\text{n of pixels with detectable CI-cyano}}{\text{n of all valid pixels}} \tag{1}$$

2.6. Quantifying effect size at all resolvable drinking water source waters

To quantify effect size at all resolvable drinking water source waters, a γ statistic was used which is conceptually equivalent to Cohen's d and has been used for several environmental applications (Coffer and Hestir,

2019; Henson et al., 2010; Urquhart et al., 2017). In this study, this statistic was used to determine the number of observations needed for a trend in the data to be sustained despite the residual variability in the data and can provide insight into how many years of data are needed to increase confidence in an observed change. If γ is less than the time period of observations, the magnitude of the trend exceeds the residual variability in the data.

To compute γ, cyanobacterial abundance values were first extracted within the previously described 900-m buffer of each drinking water intake. Cyanobacterial abundance values for all pixels contained in or intersecting this buffer were averaged for each weekly composite satellite image. Weekly averages were assigned months based on the middle day of the week, and monthly averages were computed for June 2016 through April 2020. These monthly averages were used to quantify γ at each intake, and those with a γ of less than four years were considered for a trend analysis. The γ statistic was computed following Eq. (2) as:

$$\gamma = \frac{\sqrt{\frac{\sum_1^n (y - \widehat{y})^2}{n-1}}}{|m|} \tag{2}$$

where *n* is the sample size, $\hat{y}$ represents the residuals of *y*, and *m* is the Thiel-Sen Slope.

The Thiel-Sen slope determines the magnitude of the trend by computing the slope for all pairs of data and taking their median (Sen, 1968; Theil, 1992). Relatively short time series have been used in previous studies for trend detection. Kim et al. (2007) assessed linear trends in air quality using three and five years of satellite data. Psilovikos et al. (2006) analyzed trends in water quality using three years of field observations. To assess short-term trends at each drinking water source, the nonparametric seasonal Mann Kendall test for trend and the associated Thiel-Sen slope were computed. The seasonal Mann Kendall test for trend is a variation of the Mann Kendall test for trend (Kendall, 1955; Mann, 1945), checking for a monotonic increase or decrease across the time series. The trend analysis was performed via the *rkt* package in R version 4.0.0 (Marchetto, 2017; R Core Team, 2020).

3. Results

3.1. Agreement between UCMR 4 qualitative responses and satellite observations

Of the 92 UCMR 4 qualitative responses in drinking water sources corresponding to satellite imagery, in responding to the question of whether there was an algal bloom preceding the sampling event, 8 responded "Don't know," 76 responded "No," and 8 responded "Yes." Those that responded "Yes" indicated this algal bloom was present between the day of quantitative sampling and the past month. 72 of the 76 UCMR 4 qualitative responses of "No" in drinking water sources corresponded to an absence of cyanobacteria in satellite imagery, and 7 of the 8 UCMR 4 qualitative responses of "Yes" in drinking water sources corresponded to a presence of cyanobacteria in satellite imagery (Table 1). Thus, there were five UCMR 4 qualitative responses in drinking water sources that disagreed with satellite imagery, one in which the UCMR 4 qualitative response in drinking water sources indicated a bloom was present while satellite imagery indicated a bloom

Table 1
An agreement matrix analyzing algal bloom presence and absence as indicated by UCMR 4 qualitative responses in drinking water sources and cyanobacteria detect and non-detect as indicated by satellite imagery.

UCMR 4 qualitative response	Satellite-derived cyanobacteria	
	Detect	Non-detect
Algal bloom observed	7	1
Algal bloom not observed	4	72

was absent and four in which the UCMR 4 qualitative responses in drinking water sources indicated a bloom was absent and satellite imagery indicated a bloom was present. This corresponded to an overall agreement of 94% and a Kappa coefficient of 0.70.

In addition to cyanobacterial presence and absence, the satellite-derived cyanobacterial abundance was analyzed for each of the 92 UCMR 4 qualitative responses in drinking water sources (Fig. 3). For all UCMR 4 qualitative responses in drinking water sources in which the observer did not know if an algal bloom was present, satellite imagery indicated non-detection of cyanobacteria. When UCMR 4 qualitative responses in drinking water sources indicated an algal bloom was not observed, median cyanobacterial abundance corresponded to the detection limit of the satellite imagery. When UCMR 4 qualitative responses in drinking water sources indicated an algal bloom was observed, median cyanobacterial abundance exceeded 1,200,000 cells/mL. Results of the Mann Whitney U test and associated Cohen's d indicate satellite-estimated cyanobacterial abundance corresponding to UCMR 4 qualitative responses of "Yes" and "No" are not derived from the same population ($U = 82$, $n = 84$, Cohen's $d = -4.14$). This indicates that visual observations during UCMR 4 monitoring and satellite observations have strong agreement in assessing cyanobacterial occurrence at drinking water source waters.

3.2. Bloom frequency at drinking water sources

For the year 2019, average annual bloom frequency was assessed at all 685 resolvable drinking water sources, not just those corresponding to UCMR 4 qualitative responses. For each weekly composite, an average of 19 satellite pixels were considered within a 900-m buffer of each
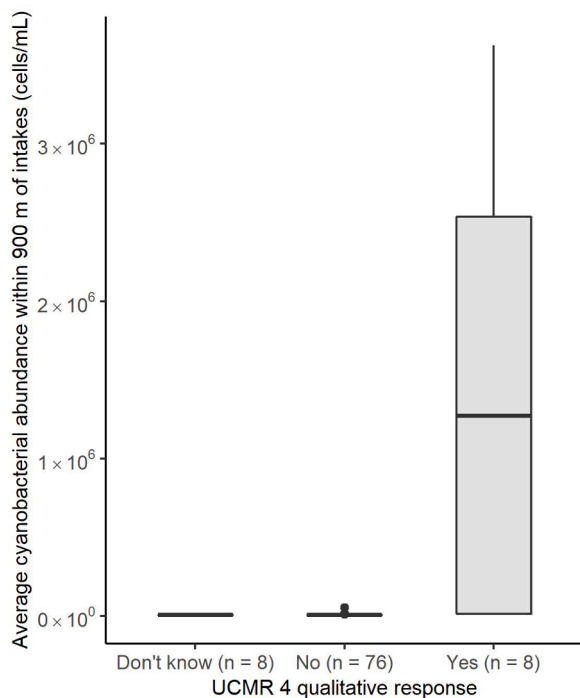

Fig. 3. Boxplots representing satellite-derived cyanobacterial abundance corresponding to fourth Unregulated Contaminant Monitoring Rule (UCMR 4) qualitative responses in drinking water sources. Gray boxes represent the 25th percentile, median, and 75th percentile; top whiskers represent 1.5 times the interquartile range from the 75th percentile; black dots represent outliers that fall outside this range. Satellite-derived cyanobacterial abundance was averaged within a 900-m buffer of drinking water intakes containing UCMR 4 data. UCMR 4 qualitative responses in drinking water sources ($n = 92$) of "Don't know," "No," and "Yes" were considered regarding whether a visible algal bloom was present within one month of quantitative sampling.

drinking water intake to compute average annual bloom frequency. Average bloom frequency in 2019 peaked at 100%, meaning that for all valid satellite pixels, the average of those closest to the intake always indicated a cyanobacterial bloom was present (Fig. 4A). Average bloom frequency reached 100% at source waters in Morgan Lake, New Mexico, and Grand Lake, Ohio (commonly referred to as Grand Lake St. Mary's), throughout the entire year in 2019. Despite relatively high average bloom frequency within 900 m at several intakes, the majority of the distribution fell below the third quartile at 13%, and the median was 2%. Outliers existed at source waters with an average frequency above 35%.

The four states with the maximum number of resolvable drinking water sources were selected to demonstrate cyanobacterial frequency in more detail (Fig. 4B); similar results can be generated for any boundary, including states, nations, or ecoregions. Texas is located in the southern United States bordering Mexico and the Gulf of Mexico. Texas's climate is characterized primarily as subtropical in its central and eastern portions and as arid desert in its western portions. New York is located in the northeast United States, sharing a border with Canada and extending to the Atlantic Ocean. New York's climate is characterized almost entirely as humid continental. California is located along the Pacific coast, and the southern portion of the state also shares a border with Mexico. Most of California is characterized as having a Mediterranean climate, but some southeastern portions of the state are characterized as desert and semi-arid. Oklahoma is located just north of Texas and its climate is primarily characterized as humid subtropical.

Texas contains 130 resolvable intakes whose statewide average bloom frequency was 18.3% in 2019, exceeding the third quartile of all resolvable intakes for the same period of time. Three source waters had an average bloom frequency of 80% in 2019 while all others were below 70%. New York contains 96 resolvable intakes which averaged the lowest statewide bloom frequency in 2019 of these four states at only 1.74%, equivalent to the median of all resolvable source waters. The resolvable source waters with the highest average bloom frequency in New York were below 20%. California contains 75 resolvable intakes that exhibited a statewide average bloom frequency of 3.26% in 2019. Two source waters had the highest average frequencies for this state with values of 50%. Over half of the resolvable source waters in California had an average bloom frequency of 0% for 2019. Oklahoma contains 71 resolvable intakes that exhibited a statewide average bloom frequency of 4.63% in 2019. The source waters that exhibited the highest average bloom frequency had a value below 50%, and many of the subsequently ranked source waters showed relatively high average bloom frequencies compared to New York and California.

3.3. Analysis of effect size at drinking water sources

Effect size was analyzed at all 685 resolvable drinking water sources, as described in Section 2.6. There were five source waters that were excluded due to low temporal coverage as they did not contain at least four observations for any given month in that time period. This left 680 resolvable source waters to include in the analysis of effect size. A trend analysis was first applied to average monthly frequencies, but no source waters had an effect size indicative of a sustained change (i.e., $\gamma \leq 4$ years), so this metric was not considered further. Instead, a trend analysis was applied to average satellite-derived cyanobacterial abundance values (cells/mL). Thus, results presented here indicate changes in satellite-derived cyanobacterial abundance estimates; more data would be needed to identify changes in temporal frequency.

A time period of four years did not provide sufficient cyanobacterial abundance data to determine a sustained trend amid inherent variability in the data for nearly all resolvable source waters. Based on the observed variability, a median temporal data collection period of just over a decade would be needed to assess trends, given the same sampling frequency (Fig. 5). The nature of the γ statistic requires a detectable slope in order for this statistic to be quantified, and a relatively small slope will
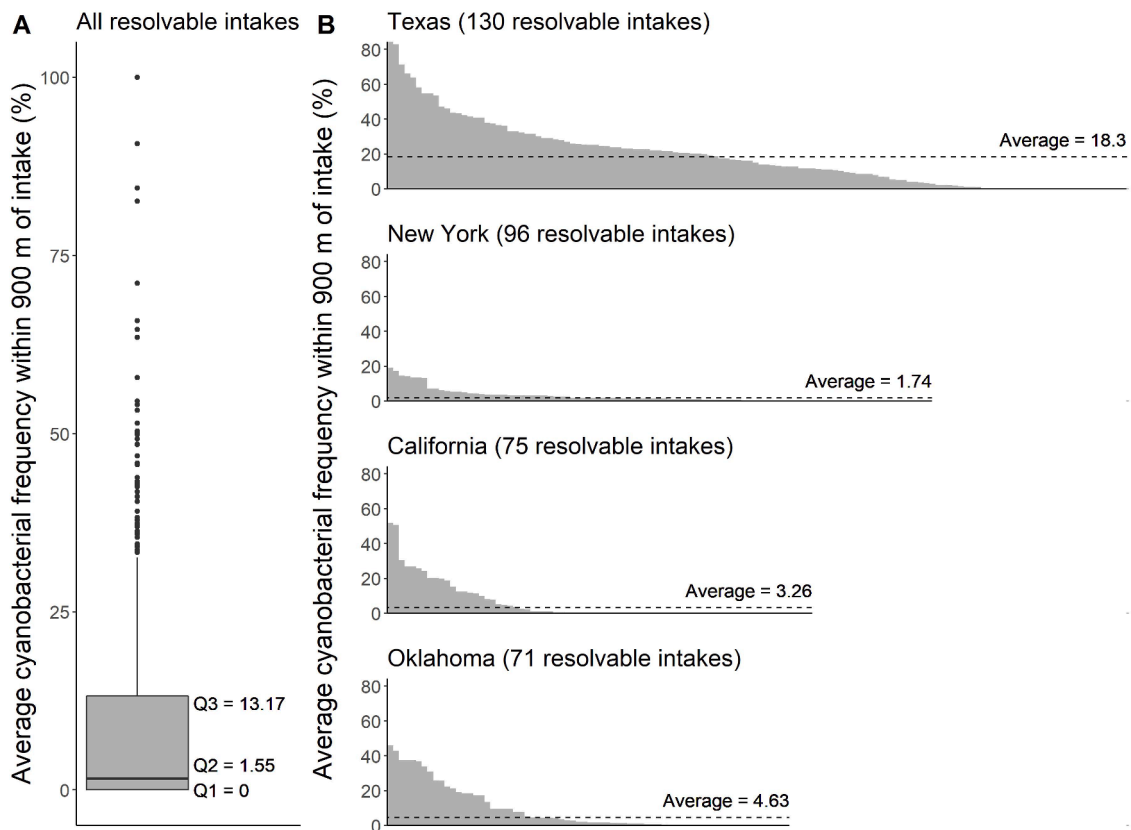
Fig. 4. (A) Distribution of average cyanobacterial bloom frequency for 2019 within 900 m of all 685 resolvable drinking water intakes across the United States. Gray boxes represent the 25th percentile, median, and 75th percentile; top whiskers represent 1.5 times the interquartile range from the 75th percentile; black dots represent outliers that fall outside this range. (B) Average cyanobacterial bloom frequency for 2019 within 900 m of resolvable drinking water intakes in the states of Texas, New York, California, and Oklahoma. The length of the x-axis reflects the number of resolvable intakes in each state. Average bloom frequency for all resolvable source waters in each state is represented by the dashed line.

result in a very large γ. Thus, a cutoff on γ of 50 years was selected for Fig. 5 to focus the analysis on more achievable monitoring time periods, which resulted in a subset of 36 intakes being selected for computing the median γ statistic.

Five source waters did exhibit an effect size indicative of a sustained trend from June 2016 through April 2020 (γ ≤ 4 years), but conclusions cannot be drawn regarding changes that may have occurred outside of this time period (Table 2, Fig. 6). Source waters at Morgan Lake in New Mexico (NM) increased in average cyanobacterial abundance by 60% per year from 2016 to 2020, and a γ of 3 years indicates that this increase represents a sustained trend. Source waters at Lake Overholser in Oklahoma (OK), Grand Lake in Ohio (OH), Choke Canyon Reservoir in Texas (TX), and Lake Eufaula, OK, decreased in cyanobacterial abundance from 2016 to 2020. Lake Overholser, OK, decreased by 30% per year and exhibited the lowest γ of the entire dataset, requiring only 1 year of observations to draw a conclusion about the observed trend. Grand Lake, OH, decreased in cyanobacterial abundance by only 10% per year, but the γ statistic still supported a sustained trend requiring 3 years of data. Both Choke Canyon Reservoir, TX, and Lake Eufaula, OK, decreased by 20% per year and required 3 years of observations for the trend to overcome residual variability in the data.

4. Discussion

4.1. Comparison of satellite-derived data with field observations

This study serves as the first quantitative comparison between satellite remote sensing data and UCMR 4 qualitative responses, providing an assessment of two independent approaches for assessing the presence

of cyanobacterial blooms in drinking water sources. Agreement between UCMR 4 qualitative responses in drinking water sources of algal presence and satellite-derived cyanobacterial abundances increases confidence in both the accuracy of PWS samplers' visual interpretation of algal blooms and the use of satellite imagery for detecting cyanobacteria at surface source waters. A Kappa coefficient of 0.70 was found between the two datasets. Kappa coefficients between 0.60 and 0.79 are considered to have a moderate level of agreement (McHugh, 2012).

While 79 responses agreed between the two datasets, there were five disagreements. However, in the absence of field measured cyanobacterial abundance, discrepancies between satellite-estimated cyanobacterial presence and UCMR 4 qualitative responses cannot be reconciled with complete certainty. In four cases, UCMR 4 qualitative responses in drinking water sources recorded no visual observation of an algal bloom, but corresponding satellite measurements indicated cyanobacteria detections were present. At these four cases, at least one of the pixels extracted within a 900-m buffer of the intake had a non-detect, but other pixels within the 900-m buffer did have detects, resulting in the aggregation of these pixels indicating cyanobacteria presence. Thus, the discrepancy could partially be explained by spatial mismatches between the exact visual observations and the 900-m buffer. Additionally, temporal offset between the two datasets could exist.

In one case, UCMR 4 qualitative responses in drinking water sources recorded a bloom, but corresponding satellite measurements indicated non-detect. For this sample, the UCMR 4 qualitative response in drinking water sources to the question "Preceding the finished water sample collection, did you observe an algal bloom in your source waters near the intake?" was that an algal bloom was observed between the past week and past month. A temporal offset could explain this discrepancy,
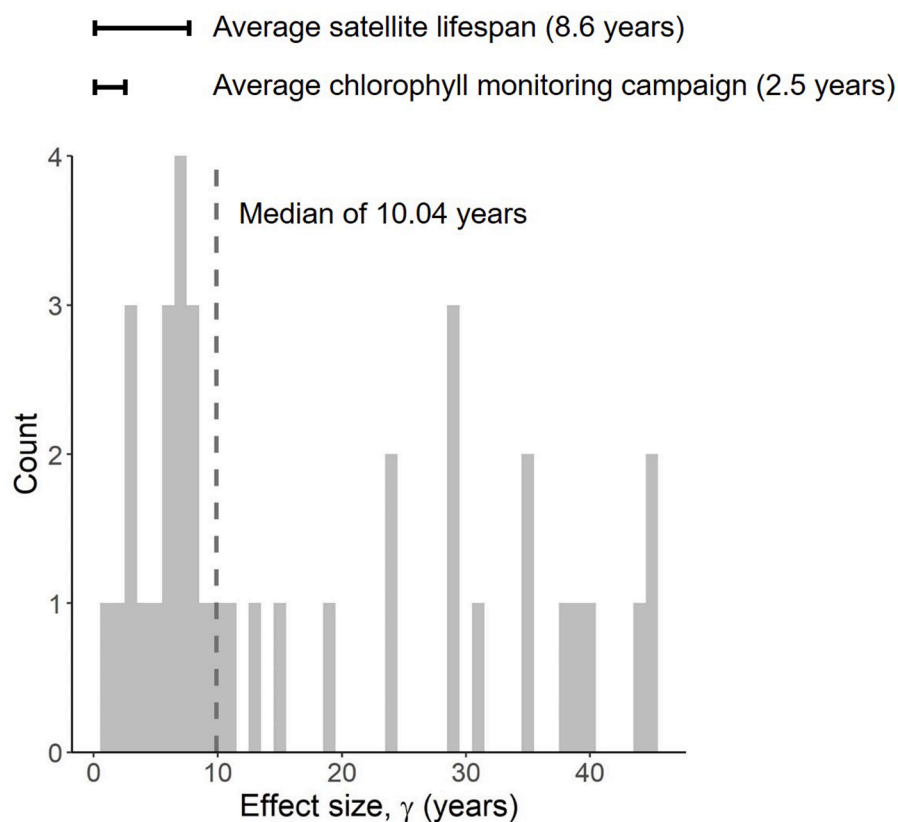
Fig. 5. A histogram of the effect size (γ) representing the length of observations needed for the current trend to exceed the residual variability at 36 source waters, selected based on a γ of less than 50 years. The median γ value was 10.04 years based on current sampling frequency. This value is slightly higher than the average satellite lifespan from the 1990′s of 8.6 years (Belward and Skøien, 2015) and nearly 8 years longer than the average water quality field campaign for chlorophyll measurements based on information from the Water Quality Portal (https://www.waterqualitydata.us). Chlorophyll monitoring was used as a proxy for cyanobacteria monitoring as field monitoring for cyanobacteria typically does not report results to larger databases and is only available at the state or local level.

Table 2

Results of a short-term trend analysis using satellite imagery at five drinking water sources that exhibited a sustained trend ($\gamma \leq 4$ years) based on monthly observations spanning June 2016 through April 2020; effect size is expressed in years. A negative change indicates a decrease in cyanobacterial frequency over the time period considered.

Lake	Sample size	Kendall's tau	Percent change per year	Effect size (γ)
Morgan Lake, NM	47	0.4	60%	3
Lake Overholser, OK	47	−0.7	−30%	1
Grand Lake, OH	40	−0.7	−10%	3
Choke Canyon Reservoir, TX	47	−0.4	−20%	3
Lake Eufaula, OK	47	−0.5	−20%	3

or a bloom could have been present below the detection limit of the satellite sensor. Additionally, it is possible to have cyanobacteria with no detectable surface bloom, particularly given that cyanobacteria can move horizontally and vertically throughout the water column within hours (Qi et al., 2018; Qin et al., 2018). A surface bloom could have been present at the time of UCMR 4 data collection but not at the time of satellite overpass as it may have moved within the water column. Moreover, the ability of the satellite to detect picocyanobacteria is still uncertain; picocyanobacteria could have been observed during UCMR 4 data collection, but not registered through the CI-cyano algorithm (Śliwińska-Wilczewska et al., 2018).

4.2. Large-scale assessments of cyanobacterial frequency at source waters

Monitoring and assessment of cyanobacterial blooms has not been routinely conducted in a nationally consistent manner with adequate spatial and temporal resolutions. Infrequent field monitoring has been conducted at the national level, including the National Lakes Assessment

(NLA) occurring every five years in the United States (Blocksom et al., 2016). Regional field monitoring has also been conducted, including across 142 Chinese lakes and reservoirs over two multi-year periods (Huang et al., 2020). Field monitoring can be both time- and cost-intensive, while satellite observations offer the potential for increased temporal and spatial resolutions when lakes are of sufficient size and in the absence of cloud cover or snow and ice (e.g., Coffer et al., 2020, 2021; Duan et al., 2017; Zhang et al., 2017).

Results presented here indicate that satellite imagery can be an important pre-screening tool that drinking water quality managers may use for early detection of cyanobacteria in their drinking water sources. Cost-effective and timely early detection of cyanobacteria in source waters can help inform critical treatment, monitoring, and management steps from PWSs, protecting drinking water quality from the risks posed by cyanotoxins and cyanobacteria and improving the quality of finished drinking water to ensure public health. However, field efforts such as the NLA, state, and local efforts are still needed to validate satellite observations and measure toxins and other parameters not resolvable with satellite imagery, particularly in areas not observable using satellite imagery such as the land-water interface.

Despite efforts to monitor cyanobacterial blooms across broad spatial and temporal scales, monitoring specific to drinking water sources is not routinely collected at the national level. In the United States, Clark et al. (2017) used satellite imagery from MERIS spanning 2008 through 2011 to assess cyanobacterial bloom frequency at source waters in the states of Florida and Ohio. The average cyanobacterial frequency for all resolvable source waters in Florida was 30% and for Ohio, 5%. Using a different method to extract nearby satellite pixels at each intake and using a different satellite sensor, Clark et al. (2017) found Grand Lake to have the highest temporal frequency for the state of Ohio at 83% from 2008 through 2011.

This study presents the first large-scale assessment of cyanobacterial frequency and abundance at surface drinking water intakes across the United States. National-level assessments of cyanobacterial occurrence
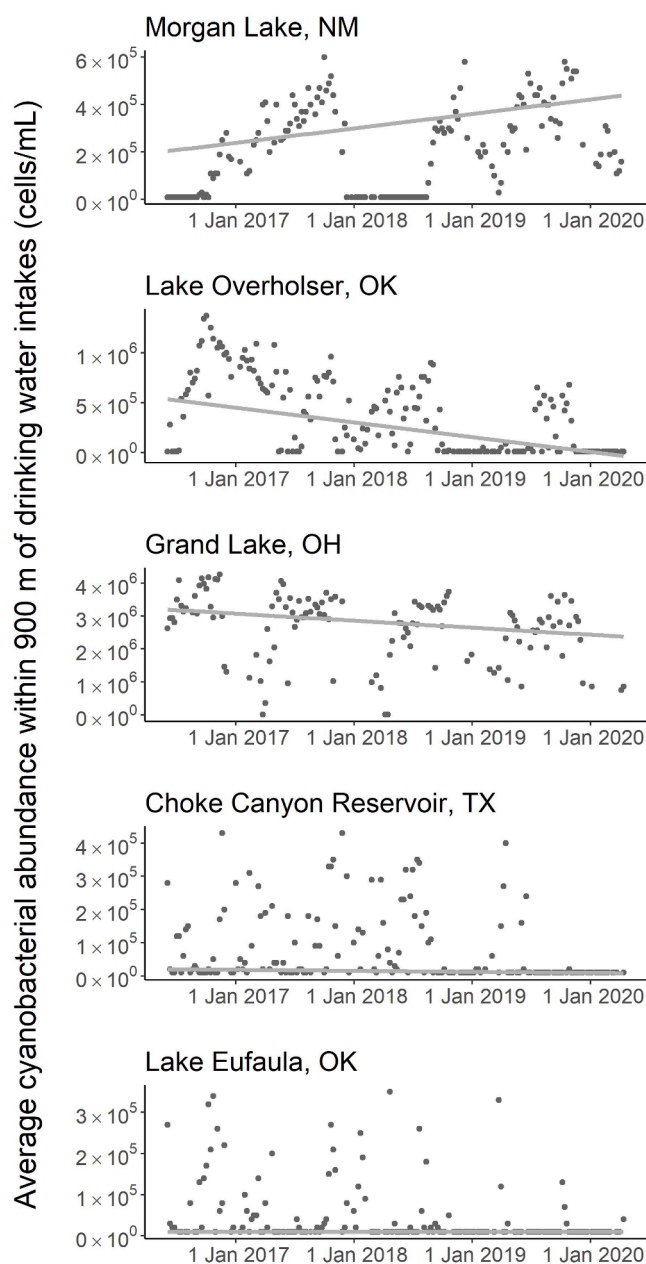
Fig. 6. Time series of average cyanobacterial abundance within 900 m of the drinking water intakes at Morgan Lake, NM; Lake Overholser, OK; Grand Lake, OH; Choke Canyon Reservoir, TX; and Lake Eufaula, OK. These five drinking water sources had an effect size less than the time period of observations ($\gamma \leq 4$ years) and were thus considered to have a sustained trend. The gray line represents the Thiel-Sen slope accompanying the change detection.

at drinking water sources have not been conducted through either field or satellite observations. Upon completion of data reporting, UCMR 4 will serve as the first field-based dataset of cyanobacteria in source waters across the United States, while methods presented here can be used to monitor approximately 700 drinking water sources across 44 states with consistent temporal coverage in the absence of cloud contamination or snow and ice cover.

4.3. Assessing effect size of cyanobacterial abundance

Anderson et al. (2002) indicated coastal systems in recent decades had increased in occurrence of toxic and otherwise harmful algal blooms, but did not provide quantitative evidence of this change. It was noted, however, that this increase could either reflect heightened scientific awareness or an actual increase in the number, magnitude, or frequency of blooms (Anderson, 1989). A lack of historical data was cited as a limitation for quantifying long-term change. He et al. (2016) also indicated the frequency of cyanobacterial blooms in freshwater systems is increasing. More recently, Huisman et al. (2018) summarized projected increases in cyanobacterial occurrence due to eutrophication, rising carbon dioxide levels, and changing climatic conditions. Despite repeated suggestions that cyanobacterial blooms have or will increase, few large-scale trend analyses have been performed to support this claim.

Using over 200 years of sediment cores from northern hemisphere lakes, Taranu et al. (2015) suggested that cyanobacteria have increased substantially in almost 60% of lakes since the industrial revolution and that cyanobacteria have increased disproportionally compared to other phytoplankton. Using satellite imagery, Urquhart et al. (2017) analyzed changes in the spatial extent of cyanobacterial blooms from 2008 through 2011 for large lakes in the states of California, Ohio, and Florida. Florida data indicated an increase in spatial extent of blooms but exhibited a γ of 4.1 over the 4-year time series, suggesting the observed trend did not quite statistically outweigh residual variability in the data.

This study found that a median of over 10 years of observations was needed for observed changes to show a sustained trend outside of the residual variability in the data given current sampling frequency. For reference, the average satellite lifespan was 8.6 years in the 1990′s (Belward and Skøien, 2015) and the average water quality field campaign for chlorophyll monitoring lasts approximately 2.5 years. Belward and Skøien (2015) also summarized satellite lifespans for more recent decades, but these values were artificially reduced given that many of the sensors considered were at the beginning of their life cycles. The average length of water quality field monitoring was found by averaging the difference between start years and end years for all Water Quality Portal (https://www.waterqualitydata.us) datasets with a characteristic name "chlorophyll." Chlorophyll monitoring was used as a proxy for cyanobacteria monitoring as field measurements for cyanobacteria are often only available through state or local databases (U.S. EPA, 2020).

OLCI completed its fourth full year of data collection in June 2020. The operational lifespan of Sentinel-3A is set to 7 years with consumables available for up to 12 years. An identical sensor is housed on ESA's Sentinel-3B satellite platform, launched in 2018. Moving forward, ESA plans to ensure consistent, long-term coverage through the launch of Sentinel-3C and Sentinel-3D. Upon successful launch of all four satellites in the Sentinel-3 satellite series, mission continuity will then be expected for at least 25 years from the launch of Sentinel-3A. Thus, the Sentinel-3 satellite constellation offers promise for providing sufficient temporal coverage for defensible, quantitative drinking water source trend assessment.

Schaeffer et al. (2013) found that mission continuity is critical for end-users. Findings here also highlight the importance of long-term monitoring programs, both satellite-based and field campaigns, in order to defend or refute statements regarding large-scale changes in cyanobacterial frequency, extent, and abundance. Insufficient temporal coverage was a primary concern for this study with nearly all drinking water sources failing to achieve a γ less than the time period of observations. Additionally, the median required time period of 10.04 years was based on an assumed sampling frequency and could be longer if the frequency of observations decreases compared to the reference 2016 through 2020 period used here. This supports the need for continued, consistent monitoring to better understand long-term cyanobacterial bloom trends in drinking water sources. The planned constellation of Sentinel-3 satellites is expected to improve temporal coverage in the future.

Despite the need for increased temporal coverage, source waters at five intakes did exhibit a sustained trend from 2016 to 2020, but these

trends cannot be extrapolated outside of this time period and are not indicative of ongoing changes. Morgan Lake is located on the Navajo Nation in northwest New Mexico. This source water exhibited the highest possible bloom frequency and was the only source water considered to increase in abundance. Lake Overholser is located in Oklahoma City, OK, and decreased in cyanobacterial abundance from 2016 to 2020. Grand Lake in western Ohio once ranked in the 99th percentile for microcystins in the United States (U.S. EPA, 2009). While Jacquemin et al. (2018) found substantial improvements in water quality over the past decade, they concluded that this lake's waters remained impaired. Choke Canyon Reservoir in southern Texas provides drinking water for the City of Corpus Christi, and Lake Eufaula, Oklahoma's largest lake, provides drinking water to Eufaula, OK. At both of these source waters, changes were driven by much lower cyanobacterial abundance values in the last year of observations compared to the first three years. Temporal patterns at these sites resembled more of a step change rather than a continuous trend, but insufficient information exists to determine a potential cause of the sudden decline in cyanobacterial abundances. At all sites, additional information would be needed to determine drivers of these changes given the short time period considered.

4.4. Limitations

While this study offers the first large-scale investigation of cyanobacterial frequency and abundance at drinking water sources across the United States, there are several limitations that warrant consideration. Only drinking water intakes located in or near relatively large lakes were considered, and pixels that fell along the shoreline were discarded, meaning approximately 80% of all drinking water intakes were not studied. When considering a subset of these drinking water intakes for matching with UCMR 4 qualitative responses in drinking water sources, coverage was even lower as UCMR 4 sampling was ongoing through the end of 2020. This study only considered UCMR 4 data reported up to April 2020 and represented a portion of data collected up to November 2019. The estimated PWS locations are based on the best available locational data provided by the states in SDWIS and are chosen to represent a PWS for this national-scale analysis. In some cases, this may cause discrepancies given the 100-m buffer used to assign a lake to each intake. Applying a similar analysis to finer resolution sensors such as Sentinel-2 at 20-m multispectral resolution or Landsat-8 at 30-m multispectral resolution could improve spatial coverage. Sentinel-2 has the potential for quantifying chlorophyll (Gilerson et al., 2010; Pahlevan et al., 2020), and Landsat has shown promise for bloom monitoring (Ho et al., 2017; Oyama et al., 2015), but cyanobacteria-specific algorithms have yet to be validated for large-scale applications. The MERIS sensor onboard ESA's Envisat can also be useful for retrospective analysis, with imagery available from 2002 through 2012.

A 900-m buffer was selected to characterize source waters at each drinking water intake. This distance was chosen to include three, 300-m satellite pixels surrounding each intake. However, these pixels do not perfectly capture the source waters influencing each drinking water intake. To determine which 300-m pixels best characterize source waters at each drinking water intake, information regarding the bathymetry, depth of each intake, and the drawdown rate would be required as well as hydrodynamic modeling specific to each system. This information is unavailable across all 685 intakes, and, therefore, it is impossible to properly identify which satellite pixels are contributing to drinking water at any given time. Thus, a generalized buffer of 900 m was chosen for consistency across locations and time.

Satellite observations of cyanobacterial frequency or abundance do not represent levels in finished drinking water. When investigating cyanobacterial abundance near these intakes, it is important to remember that this analysis focuses on source waters only. The quality of finished drinking water is a reflection of treatment practices used by the PWS in response to changes in intake water quality. For example, a

2016 report found 43.9% of source waters in Ohio to exceed the U.S. EPA Health Advisory level of 0.3 µg/L total microcystins for children and vulnerable populations, but only 1.16% of treated drinking water samples exceeded this threshold (AWWA, 2016), demonstrating effective treatment practices for the intakes considered. Moreover, satellite imagery can only detect cyanobacteria, not the presence of cyanotoxins (Stumpf et al., 2016a), and it is possible for both a visible bloom to be present without cyanotoxins and cyanotoxins to be present without a visible bloom. This issue is further complicated by the presence and the possibility of the growth and regrowth of cyanobacteria within the treatment utility, potentially leading to toxin or taste and odor production even in the absence of a bloom in the source water (Almuhtaram et al., 2018; Greenstein et al., 2020).

Several limitations exist in the acquisition of satellite imagery. Data gaps exist due to cloud cover, Sun glint contamination, and the presence of snow and ice. Northern latitude regions are particularly affected by lower data coverage in the winter months (Coffer et al., 2020), although during the cold season proliferation of cyanobacterial blooms is believed to be more limited (Ibelings et al., 2021). However, occasional blooms and in some cases cyanotoxins have been noted under ice (Bertilsson et al., 2013; Hampton et al., 2017; Üveges et al., 2012; Wejnerowski et al., 2018). Satellite images are acquired mid-day and only characterize cyanobacteria at the time of image acquisition. However, cyanobacterial blooms can change throughout the day and from one day to another. The weekly composites used here preserve the week's maximum CI-cyano value in an effort to capture any cyanobacterial bloom that may have occurred, but no information can be gathered or inferred outside the time of satellite image acquisition. Additionally, difficulties can arise in performing short-term trend analyses given limited observations.

Satellites typically cannot detect benthic cyanobacteria except in the case of optically shallow water. However, benthic systems can contribute to contamination of drinking water sources (Gaget et al., 2017). Moreover, drinking water intakes can be located at a water's surface or at depths of up to 30 to 40 m (Hoeger et al., 2005), but the satellite signal only represents the top layer of the water column, typically up to 2 m for red spectral bands in clear water (Mishra et al., 2005) and less than 2 m in more turbid waters (Wynne et al., 2010). This vertical offset can be important if using this information to inform drinking water management approaches. A vertical offset is not accounted for here and is difficult to address given that some facilities have multiple intake depths to accommodate changes in water level and water quality (U.S. EPA, 2016a).

5. Conclusions

This study used satellite imagery to detect cyanobacteria at nearly 700 drinking water sources across the United States. Additionally, agreement between a subset of 22 of these source waters and visual observations extracted from UCMR 4 qualitative responses indicating the presence or absence of a visible surface algal bloom was analyzed. The following conclusions were reached:

- A subset of UCMR 4 qualitative responses in drinking water sources spanning March 2018 through November 2019 and corresponding satellite-derived cyanobacteria detect and non-detect measurements achieved an overall agreement of 94% and a Kappa coefficient of 0.70 across 84 observations. This demonstrates the utility for use of satellite imagery as a complement to ground-based measurements for assessing cyanobacterial occurrence at drinking water sources.
- Across all resolvable drinking water sources, the majority of detectable cyanobacterial bloom frequencies for 2019 averaged less than 35%, but several outliers existed at higher frequencies reaching a maximum value of 100% for source waters at two drinking water intakes.

- Nearly all source waters analyzed did not have sufficient data for a trend analysis, as indicated by effect size statistics that were longer than the time period of observations. Instead, a decade of observations would be needed, on average, for trends to outweigh residual variability in the data.
- Five source waters demonstrated a short-term trend from June 2016 through April 2020 with source waters at one intake increasing in cyanobacterial abundance over this time period and source waters at four intakes decreasing in cyanobacterial abundance. However, conclusions are only valid within the observed time period and cannot be extrapolated to support long-term trends at any source waters. Additional data are needed to determine drivers of these changes.

Declaration of Competing Interest

The authors declare that they have no known competing financial interests or personal relationships that could have appeared to influence the work reported in this paper.

References

Almuhtaram, H., Cui, Y., Zamyadi, A., Hofmann, R., 2018. Cyanotoxins and Cyanobacteria cell accumulations in drinking water plants with a low risk of bloom formation at the source. Toxins (Basel) 10, 430. https://doi.org/10.3390/toxins10110430.

Anderson, D.M., 1989. Toxic algal blooms and red tides: a global perspective. Red tides Biol. Environ. Sci. Toxicol. 11–16.

Anderson, D.M., Glibert, P.M., Burkholder, J.M., 2002. Harmful algal blooms and eutrophication: nutrient sources, composition, and consequences. Estuaries 25, 704–726. https://doi.org/10.1007/BF02804901.

AWWA, 2016. Cyanotoxins in US Drinking Water: Occurrence, Case Studies and State Approaches to Regulation. Denver, CO.

Belward, A.S., Skøien, J.O., 2015. Who launched what, when and why; trends in global land-cover observation capacity from civilian earth observation satellites. ISPRS J. Photogramm. Remote Sens. 103, 115–128. https://doi.org/10.1016/j.isprsjprs.2014.03.009.

Bertilsson, S., Burgin, A., Carey, C.C., Fey, S.B., Grossart, H.-P., Grubisic, L.M., Jones, I. D., Kirillin, G., Lennon, J.T., Shade, A., Smyth, R.L., 2013. The under-ice microbiome of seasonally frozen lakes. Limnol. Ocean. 58 https://doi.org/10.4319/lo.2013.58.6.1998.

Blocksom, K., Kaufmann, P., Kincaid, T., Olsen, T., Paulsen, S., Peck, D., Stoddard, J., Sickle, J.Van, Weber, M., Holdsworth, S., Landis, M., Lehmann, S., Mitchell, R., Soo-Hoo, M., 2016. National lakes assessment 2012.

Clark, J.M., Schaeffer, B.A., Darling, J.A., Urquhart, E.A., Johnston, J.M., Ignatius, A.R., Myer, M.H., Loftin, K.A., Werdell, P.J., Stumpf, R.P., 2017. Satellite monitoring of cyanobacterial harmful algal bloom frequency in recreational waters and drinking water sources. Ecol. Indic. 80, 84–95. https://doi.org/10.1016/j.ecolind.2017.04.046.

Coffer, M.M., Hestir, E.L., 2019. Variability in trends and indicators of CO2 exchange across Arctic Wetlands. J. Geophys. Res. Biogeosci. 124, 1248–1264. https://doi.org/10.1029/2018JG004775.

Coffer, M.M., Schaeffer, B.A., Darling, J.A., Urquhart, E.A., Salls, W.B., 2020. Quantifying national and regional cyanobacterial occurrence in US lakes using satellite remote sensing. Ecol. Indic. 111, 105976 https://doi.org/10.1016/j.ecolind.2019.105976.

Coffer, M.M., Schaeffer, B.A., Salls, W.B., Urquhart, E.A., Loftin, K.A., Stumpf, R.P., Werdell, P.J., Darling, J.A., 2021. Satellite remote sensing to assess cyanobacterial bloom frequency across the United States at multiple spatial scales. Ecol. Indic. 128 https://doi.org/10.1016/j.ecolind.2021.107822.

Cohen, J., 1992. A power primer. Psychol. Bull. 112, 155. https://doi.org/10.1037//0033-2909.112.1.155.

Cohen, J., 1960. A coefficient of agreement for nominal scales. Educ. Psychol. Meas. 20, 37–46. https://doi.org/10.1177/001316446002000104.

Dekker, A.G., Hestir, E.L., 2012. Evaluating the feasibility of systematic inland water quality monitoring with satellite remote sensing. Commonw. Sci. Ind. Res. Organ. Canberra, Aust.

Dieter, C.A., Maupin, M.A., Caldwell, R.R., Harris, M.A., Ivahnenko, T.I., Lovelace, J.K., Barber, N.L., Linsey, K.S., Survey, U.S.G., 2018. Estimated use of water in the United States in 2015. U.S. Geol. Surv. Circular 1441. https://doi.org/10.3133/cir1441.

Duan, H., Tao, M., Loiselle, S.A., Zhao, W., Cao, Z., Ma, R., Tang, X., 2017. MODIS observations of cyanobacterial risks in a eutrophic lake: implications for long-term safety evaluation in drinking-water source. Water Res. 122, 455–470. https://doi.org/10.1016/j.watres.2017.06.022.

Gaget, V., Humpage, A., Huang, Q., Monis, P., Brookes, J., 2017. Benthic cyanobacteria: a source of cylindrospermopsin and microcystin in Australian drinking water reservoirs. Water Res. 124 https://doi.org/10.1016/j.watres.2017.07.073.

Gilerson, A.A., Gitelson, A.A., Zhou, J., Gurlin, D., Moses, W., Ioannou, I., Ahmed, S.A., 2010. Algorithms for remote estimation of chlorophyll-a in coastal and inland waters using red and near infrared bands. Opt. Express 18, 24109–24125.

GLCR, 2013. Microcystis Outbreak Closes Lake Erie Water Treatment Plant.

Goodman, L.A., Kruskal, W.H., 1954. Measures of association for cross classifications. J. Am. Stat. Assoc. 49, 732–764. https://doi.org/10.1080/01621459.1954.10501231.

Gower, J., King, S., Borstad, G., Brown, L., 2005. Detection of intense plankton blooms using the 709 nm band of the MERIS imaging spectrometer. Int. J. Remote Sens. 26, 2005–2012. https://doi.org/10.1080/01431160500075857.

Graham, J.L., Loftin, K.A., Ziegler, A.C., Meyer, M.T., 2008. Guidelines for Design and Sampling For Cyanobacterial Toxin and Taste-And-Odor Studies in Lakes and Reservoirs. U. S. Geological Survey.

Great Lakes Commission, 2014. City of Toledo Drinking Water Advisory and Ohio EPA Response to Harmful Algal Blooms.

Greenstein, K.E., Zamyadi, A., Glover, C.M., Adams, C., Rosenfeldt, E., Wert, E.C., 2020. Delayed release of intracellular microcystin following partial oxidation of cultured and naturally occurring Cyanobacteria. Toxins (Basel) 12, 335. https://doi.org/10.3390/toxins12050335.

Hampton, S.E., Galloway, A.W.E., Powers, S.M., Ozersky, T., Woo, K.H., Batt, R.D., Labou, S.G., O'Reilly, C.M., Sharma, S., Lottig, N.R., Stanley, E.H., North, R.L., Stockwell, J.D., Adrian, R., Weyhenmeyer, G.A., Arvola, L., Baulch, H.M., Bertani, I., Bowman, L.L., Carey, C.C., Catalan, J., Colom-Montero, W., Domine, L.M., Felip, M., Granados, I., Gries, C., Grossart, H.-P., Haberman, J., Haldna, M., Hayden, B., Higgins, S.N., Jolley, J.C., Kahilainen, K.K., Kaup, E., Kehoe, M.J., MacIntyre, S., Mackay, A.W., Mariash, H.L., McKay, R.M., Nixdorf, B., Nõges, P., Nõges, T., Palmer, M., Pierson, D.C., Post, D.M., Pruett, M.J., Rautio, M., Read, J.S., Roberts, S. L., Rücker, J., Sadro, S., Silow, E.A., Smith, D.E., Sterner, R.W., Swann, G.E.A., Timofeyev, M.A., Toro, M., Twiss, M.R., Vogt, R.J., Watson, S.B., Whiteford, E.J., Xenopoulos, M.A., 2017. Ecology under lake ice. Ecol. Lett. 20, 98–111. https://doi.org/10.1111/ele.12699.

He, X., Liu, Y.L., Conklin, A., Westrick, J., Weavers, L.K., Dionysiou, D.D., Lenhart, J.J., Mouser, P.J., Szlag, D., Walker, H.W., 2016. Toxic cyanobacteria and drinking water: impacts, detection, and treatment. Harmful Algae 54, 174–193. https://doi.org/10.1016/j.hal.2016.01.001.

Henson, S.A., Sarmiento, J.L., Dunne, J.P., Bopp, L., Lima, I., Doney, S.C., John, J., Beaulieu, C., 2010. Detection of anthropogenic climate change in satellite records of ocean chlorophyll and productivity. Biogeosciences 7, 621–640. https://doi.org/10.5194/bg-7-621-2010.

Ho, J.C., Stumpf, R.P., Bridgeman, T.B., Michalak, A.M., 2017. Using Landsat to extend the historical record of lacustrine phytoplankton blooms: a Lake Erie case study. Remote Sens. Environ. 191, 273–285. https://doi.org/10.1016/j.rse.2016.12.013.

Hoeger, S.J., Hitzfeld, B.C., Dietrich, D.R., 2005. Occurrence and elimination of cyanobacterial toxins in drinking water treatment plants. Toxicol. Appl. Pharmacol. 203, 231–242.

Hu, C., 2009. A novel ocean color index to detect floating algae in the global oceans. Remote Sens. Environ. 113, 2118–2129.

Huang, J., Zhang, Y., Arhonditsis, G.B., Gao, J., Chen, Q., Peng, J., 2020. The magnitude and drivers of harmful algal blooms in China's lakes and reservoirs: a national-scale characterization. Water Res. 181, 115902 https://doi.org/10.1016/j.watres.2020.115902.

Huisman, J., Codd, G.A., Paerl, H.W., Ibelings, B.W., Verspagen, J.M.H., Visser, P.M., 2018. Cyanobacterial blooms. Nat. Rev. Microbiol. 16, 471–483. https://doi.org/10.1038/s41579-018-0040-1.

Hunter, P.D., Tyler, A.N., Gilvear, D.J., Willby, N.J., 2009. Using remote sensing to aid the assessment of human health risks from blooms of potentially toxic cyanobacteria. Environ. Sci. Technol. 43, 2627–2633.

Ibelings, B.W., Kurmayer, R., Azevedo, S.M.F.O., Wood, S.A., Chorus, I., Welker, M., 2021. Understanding the occurrence of cyanobacteria and cyanotoxins. Toxic Cyanobacteria in Water. CRC Press, pp. 213–294.

Jacquemin, S.J., Johnson, L.T., Dirksen, T.A., McGlinch, G., 2018. Changes in water quality of Grand Lake St. Marys watershed following implementation of a distressed watershed rules package. J. Environ. Qual. 47, 113–120. https://doi.org/10.2134/jeq2017.08.0338.

Jin, Q., Lyu, H., Shi, L., Miao, S., Wu, Z., Li, Y., Wang, Q., 2017. Developing a two-step method for retrieving cyanobacteria abundance from inland eutrophic lakes using MERIS data. Ecol. Indic. 81, 543–554. https://doi.org/10.1016/j.ecolind.2017.06.027.

Kahru, M., Elmgren, R., 2014. Multidecadal time series of satellite-detected accumulations of cyanobacteria in the Baltic Sea. Biogeosciences 11, 3619.

Kendall, M.G., 1955. Rank Correlation Methods, 2nd ed. Hafner Publishing Co., Oxford, England.

Kim, S.-.W., Heckel, A., Frost, G., Richter, A., Gleason, J., Burrows, J., McKeen, S., Hsie, E.-.Y., Granier, C., Trainer, M., 2007. NO2 columns in the western United States observed from space and simulated by a regional chemistry model and their implications for NOx emissions. J. Geophys. Res. 114, D11301. https://doi.org/10.1029/2008JD011343.

Kutser, T., 2009. Passive optical remote sensing of cyanobacteria and other intense phytoplankton blooms in coastal and inland waters. Int. J. Remote Sens. 30, 4401–4425. https://doi.org/10.1080/01431160802562305.

Kutser, T., Metsamaa, L., Strömbeck, N., Vahtmäe, E., 2006. Monitoring cyanobacterial blooms by satellite remote sensing. Estuar. Coast. Shelf Sci. 67, 303–312.

Lunetta, R., Schaeffer, B.A., Stumpf, R.P., Keith, D., Jacobs, S.A., Murphy, M.S., 2015. Evaluation of cyanobacteria cell count detection derived from MERIS imagery across the eastern USA. Remote Sens. Environ. 157, 24–34. https://doi.org/10.1016/j.rse.2014.06.008.

Mann, H.B., 1945. Nonparametric tests against trend. Econometrica 13, 245–259. https://doi.org/10.2307/1907187.

Mann, H.B., Whitney, D.R., 1947. On a test of whether one of two random variables is stochastically larger than the other. Ann. Math. Stat. 18, 50–60. https://doi.org/10.1214/AOMS/1177730491.

Marchetto, A., 2017. rkt: Mann-Kendall Test, Seasonal and Regional Kendall Tests.

Matthews, M.W., Bernard, S., 2015. Eutrophication and cyanobacteria in South Africa's standing water bodies: a view from space. S. Afr. J. Sci. 111, 1–8.

Matthews, M.W., Bernard, S., Robertson, L., 2012. An algorithm for detecting trophic status (chlorophyll-a), cyanobacterial-dominance, surface scums and floating vegetation in inland and coastal waters. Remote Sens. Environ. 124, 637–652. https://doi.org/10.1016/j.rse.2012.05.032.

Matthews, M.W., Odermatt, D., 2015. Improved algorithm for routine monitoring of cyanobacteria and eutrophication in inland and near-coastal waters. Remote Sens. Environ. 156, 374–382. https://doi.org/10.1016/j.rse.2014.10.010.

McHugh, M.L., 2012. Interrater reliability: the kappa statistic. Biochem. Medica 22, 276–282.

Mishra, D.R., Narumalani, S., Rundquist, D., Lawson, M., 2005. Characterizing the vertical diffuse attenuation coefficient for downwelling irradiance in coastal waters: implications for water penetration by high resolution satellite data. ISPRS J. Photogramm. Remote Sens. 60, 48–64. https://doi.org/10.1016/j.isprsjprs.2005.09.003.

Mishra, S., Stumpf, R.P., Schaeffer, B.A., Werdell, P.J., Loftin, K.A., Meredith, A., 2021. Evaluation of a satellite-based cyanobacteria bloom detection algorithm using field-measured Microcystin data. Sci. Total Environ. 774 https://doi.org/10.1016/j.scitotenv.2021.145462.

Mishra, S., Stumpf, R.P., Schaeffer, B.A., Werdell, P.J., Loftin, K.A., Meredith, A., 2019. Measurement of Cyanobacterial Bloom magnitude using satellite remote sensing. Sci. Rep. 9, 18310. https://doi.org/10.1038/s41598-019-54453-y.

Moradi, M., 2014. Comparison of the efficacy of MODIS and MERIS data for detecting cyanobacterial blooms in the southern Caspian Sea. Mar. Pollut. Bull. 87, 311–322. https://doi.org/10.1016/j.marpolbul.2014.06.053.

Nakazawa, M., 2019. fmsb: Functions for Medical Statistics Book with some Demographic Data.

Oyama, Y., Fukushima, T., Matsushita, B., Matsuzaki, H., Kamiya, K., Kobinata, H., 2015. Monitoring levels of cyanobacterial blooms using the visual cyanobacteria index (VCI) and floating algae index (FAI). Int. J. Appl. Earth Obs. Geoinf. 38, 335–348.

Pace, M.L., Batt, R.D., Buelo, C.D., Carpenter, S.R., Cole, J.J., Kurtzweil, J.T., Wilkinson, G.M., 2017. Reversal of a cyanobacterial bloom in response to early warnings. Proc. Natl. Acad. Sci. 114, 352–357.

Pahlevan, N., Smith, B., Schalles, J., Binding, C., Cao, Z., Ma, R., Alikas, K., Kangro, K., Gurlin, D., Hà, N., 2020. Seamless retrievals of chlorophyll-a from Sentinel-2 (MSI) and Sentinel-3 (OLCI) in inland and coastal waters: a machine-learning approach. Remote Sens. Environ., 111604

Palmer, S.C.J., Odermatt, D., Hunter, P.D., Brockmann, C., Présing, M., Balzter, H., Tóth, V.R., 2015. Satellite remote sensing of phytoplankton phenology in Lake Balaton using 10years of MERIS observations. Remote Sens. Environ. 158, 441–452. https://doi.org/10.1016/j.rse.2014.11.021.

Papenfus, M., Schaeffer, B., Pollard, A.I., Loftin, K., 2020. Exploring the potential value of satellite remote sensing to monitor chlorophyll-a for US lakes and reservoirs. Environ. Monit. Assess. 192, 808. https://doi.org/10.1007/s10661-020-08631-5.

Psilovikos, Aris, Margoni, S., Psilovikos, Antonios, 2006. Simulation and trend analysis of the water quality monitoring daily data in Nestos River Delta. Contribution to the sustainable management and results for the years 2000–2002. Environ. Monit. Assess. 116, 543–562. https://doi.org/10.1007/s10661-006-7671-9.

Qi, L., Hu, C., Visser, P.M., Ma, R., 2018. Diurnal changes of cyanobacteria blooms in Taihu Lake as derived from GOCI observations. Limnol. Oceanogr. 63, 1711–1726. https://doi.org/10.1002/lno.10802.

Qin, B., Yang, G., Ma, J., Wu, T., Li, W., Liu, L., Deng, J., Zhou, J., 2018. Spatiotemporal changes of Cyanobacterial Bloom in large shallow eutrophic Lake Taihu. China. Front. Microbiol. 9, 451.

R Core Team, 2020. R: A Language and Environment for Statistical Computing.

Schaeffer, B.A., Bailey, S.W., Conmy, R.N., Galvin, M., Ignatius, A.R., Johnston, J.M., Keith, D.J., Lunetta, R.S., Parmar, R., Stumpf, R.P., Urquhart, E.A., Werdell, P.J., Wolfe, K., 2018. Mobile device application for monitoring cyanobacteria harmful algal blooms using Sentinel-3 satellite Ocean and Land Colour Instruments. Environ. Model. Softw. 109, 93–103. https://doi.org/10.1016/j.envsoft.2018.08.015.

Schaeffer, B.A., Schaeffer, K.G., Keith, D., Lunetta, R.S., Conmy, R., Gould, R.W., 2013. Barriers to adopting satellite remote sensing for water quality management. Int. J. Remote Sens. 34, 7534–7544. https://doi.org/10.1080/01431161.2013.823524.

Sen, P.K., 1968. Estimates of the regression coefficient based on Kendall's. Tau. J. Am. Stat. Assoc. 63, 1379–1389. https://doi.org/10.1080/01621459.1968.10480934.

Shi, K., Zhang, Y., Zhou, Y., Liu, X., Zhu, G., Qin, B., Gao, G., 2017. Long-term MODIS observations of cyanobacterial dynamics in Lake Taihu: responses to nutrient enrichment and meteorological factors. Sci. Rep. 7, 40326. https://doi.org/10.1038/srep40326.

Śliwińska-Wilczewska, S., Maculewicz, J., Barreiro Felpeto, A., Latała, A., 2018. Allelopathic and bloom-forming picocyanobacteria in a changing world. Toxins (Basel) 10, 48. https://doi.org/10.3390/toxins10010048.

Stroming, S., Robertson, M., Mabee, B., Kuwayama, Y., Schaeffer, B., 2020. Quantifying the Human health benefits of using satellite information to detect Cyanobacterial Harmful algal blooms and manage recreational advisories in U.S. Lakes. GeoHealth 4, e2020GH000254. https://doi.org/10.1029/2020GH000254.

Stumpf, R.P., Davis, T.W., Wynne, T.T., Graham, J.L., Loftin, K.A., Johengen, T.H., Gossiaux, D., Palladino, D., Burtner, A., 2016a. Challenges for mapping cyanotoxin patterns from remote sensing of cyanobacteria. Harmful Algae 54, 160–173. https://doi.org/10.1016/j.hal.2016.01.005.

Stumpf, R.P., Johnson, L.T., Wynne, T.T., Baker, D.B., 2016b. Forecasting annual cyanobacterial bloom biomass to inform management decisions in Lake Erie. J. Great Lakes Res. 42, 1174–1183. https://doi.org/10.1016/j.jglr.2016.08.006.

Szlag, D.C., Sinclair, J.L., Southwell, B., Westrick, J.A., 2015. Cyanobacteria and cyanotoxins occurrence and removal from five high-risk conventional treatment drinking water plants. Toxins (Basel) 7, 2198–2220.

Taranu, Z.E., Gregory-Eaves, I., Leavitt, P.R., Bunting, L., Buchaca, T., Catalan, J., Domaizon, I., Guilizzoni, P., Lami, A., McGowan, S., 2015. Acceleration of cyanobacterial dominance in north temperate-subarctic lakes during the Anthropocene. Ecol. Lett. 18, 375–384.

The Novak Consulting Group, 2018. City of Salem Water Advisory After-Action Assessment.

Theil, H., 1992. A rank-invariant method of linear and polynomial regression analysis. In: Raj, B., Koerts, J. (Eds.), Henri Theil's Contributions to Economics and Econometrics: Econometric Theory and Methodology. Springer, Netherlands, Dordrecht, pp. 345–381. https://doi.org/10.1007/978-94-011-2546-8_20.

Torchiano, M., 2020. effsize: Efficient Effect Size Computation. https://doi.org/10.5281/zenodo.1480624.

U.S. EPA, 2020. State HABs Monitoring Programs and Resources [WWW Document]. URL https://www.epa.gov/cyanohabs/state-habs-monitoring-programs-and-resources.

U.S. EPA, 2016a. Water treatment optimization for cyanotoxins.

U.S. EPA, 2016b. The Fourth Unregulated Contaminant Monitoring Rule (UCMR 4) General Information.

U.S. EPA, 2016c. The Fourth Unregulated Contaminant Monitoring Rule (UCMR 4) Cyanotoxins – Fact Sheet for Assessment Monitoring.

U.S. EPA, 2009. National lakes assessment: a collaborative survey of the nation's lakes.

Urquhart, E.A., Schaeffer, B.A., 2020. Envisat MERIS and Sentinel-3 OLCI satellite lake biophysical water quality flag dataset for the contiguous United States. Data Br. 28, 104826 https://doi.org/10.1016/j.dib.2019.104826.

Urquhart, E.A., Schaeffer, B.A., Stumpf, R.P., Loftin, K.A., Werdell, P.J., 2017. A method for examining temporal changes in cyanobacterial harmful algal bloom spatial extent using satellite remote sensing. Harmful Algae 67, 144–152. https://doi.org/10.1016/J.HAL.2017.06.001.

Üveges, V., Tapolczai, K., Krienitz, L., Padisák, J., 2012. Photosynthetic characteristics and physiological plasticity of an Aphanizomenon flos-aquae (Cyanobacteria, Nostocaceae) winter bloom in a deep oligo-mesotrophic lake (Lake Stechlin, Germany). Phytoplankton Responses to Human Impacts at Different Scales. Springer, Netherlands, pp. 263–272. https://doi.org/10.1007/978-94-007-5790-5_20.

Wejnerowski, Ł., Rzymski, P., Kokociński, M., Meriluoto, J., 2018. The structure and toxicity of winter cyanobacterial bloom in a eutrophic lake of the temperate zone. Ecotoxicology 27, 752–760. https://doi.org/10.1007/s10646-018-1957-x.

Wilcoxon, F., 1945. Individual comparisons by ranking methods. Biometrics Bull.

Wilkinson, G.M., Carpenter, S.R., Cole, J.J., Pace, M.L., Batt, R.D., Buelo, C.D., Kurtzweil, J.T., 2018. Early warning signals precede cyanobacterial blooms in multiple whole-lake experiments. Ecol. Monogr. 88, 188–203.

Wynne, T.T., Stumpf, R., Tomlinson, M., Dyble, J., 2010. Characterizing a cyanobacterial bloom in Western Lake Erie using satellite imagery and meteorological data. Limnol. Oceanogr. 55, 2025–2036. https://doi.org/10.4319/lo.2010.55.5.2025.

Wynne, T.T., Stumpf, R.P., Tomlinson, M.C., Warner, R.A., Tester, P.A., Dyble, J., Fahnenstiel, G.L., 2008. Relating spectral shape to cyanobacterial blooms in the Laurentian Great Lakes. Int. J. Remote Sens. 29, 3665–3672. https://doi.org/10.1080/01431160802007640.

Wyoming DEQ, 2018a. Big Sandy Reservoir Harmful Cyanobacterial Investigation 2018.

Wyoming DEQ, 2018b. Eden Reservoir Harmful Cyanobacterial Investigation 2018.

Wyoming DEQ, 2018c. Pathfinder Reservoir Harmful Cyanobacterial Bloom Investigation 2018.

Zhang, F., Hu, C., Shum, C.K., Liang, S., Lee, J., 2017. Satellite remote sensing of drinking water intakes in Lake Erie for Cyanobacteria population using two MODIS-based indicators as a potential tool for toxin tracking. Front. Mar. Sci. 4, 124.